Biomaterials Science

Quantification of Volume and Size Distribution of Internalised Calcium Phosphate Particles and Their Influence on Cell Fate

Journal:	*Biomaterials Science*
Manuscript ID:	BM-COM-07-2014-000238
Article Type:	Communication
Date Submitted by the Author:	09-Jul-2014
Complete List of Authors:	Williams, Richard; University of Birmingham, Biochemical Engineering Vizcaíno-Castón, Isaac; University of Birmingham, Biochemical Engineering Grover, Liam; University of Birmingham, Biochemical Engineering

Quantification of Volume and Size Distribution of Internalised Calcium Phosphate Particles and Their Influence on Cell Fate †

Richard L. Williams[a], Isaac Vizcaíno-Castón[a] and Liam M. Grover*[a]

Received Xth XXXXXXXXXX 20XX, Accepted Xth XXXXXXXXX 20XX
First published on the web Xth XXXXXXXXXX 200X
DOI: 10.1039/b000000x

We report preliminary findings suggesting that the diameter of the internalised calcium phosphate particles is critical to cell fate with particles/aggregates of particles of larger than 1.5μm leading to cell death. This has significant implications for the design of medical materials even from those consisting of non-toxic calcium phosphate salts.

Calcium phosphates (CaPs) have been used extensively as bone replacement materials, substrates for drug release and transfection agents[1–6] because of their non-cytotoxic nature and chemical similarity to the mineral component of human bone. There are numerous studies of CaPs of different morphology, size, surface area and zeta-potential and their effect on cellular uptake[7,8], transfection efficiency and cytoxicity[8,9]. However, the fate and precise location of the material once inside the cell, together with it's effect on the cell itself, is not fully understood. Motskin *et al.* (2009) attempted to quantify the volume of CaP within fixed human macrophages from TEM images and reported significant localisation within lysosomes from observations[8]. Together with image data, they concluded that apparent cytoxicity was dependent on the volume of the internalised material[8]. It's been widely reported that the mechanism behind this apparent cytoxicity involves the release of Ca^{2+} from the CaP structures dissolved within the acidic environment of the lysosomes[8,10], which in turn interferes with Ca^{2+} mediated signalling pathways including those involved in apoptosis[11–13]. However, it's unclear whether this calcium ion release is actually dependent purely on the total volume of the internalised CaP within the cell membrane because there are no studies to date which have quantified the amount of material within lysosomes and free in the cytosol.

We previously reported a method for the surface modification of silicon-substituted hydroxyapatite (SiHA) with thiol groups, which enabled the engraftment of a fluorescein-5-maleimide probe and hence the clear visual discrimination of the material from cells[14] (†figure S1). In this work, cellular internalisation and lysosomal processing of calcium phosphate particles by MC3T3 cells has been visualised and quantified through surface modification and fluorescent tagging along with lysosome co-labelling (†ESI section 1.1 for materials and methods). Computational image analysis of 3D confocal image stacks was used (†section 1.3) to estimate the size distribution (†Figure S2) and volume (†Figure S3) of the internalised material located both within and outside of the lysosomes. Gel electrophoresis of the labelled particles showed that the dye remained bound to the functionalised particle surface after extensive washing and that excess unbound dye had been removed (Figure S4), hence the detected fluorescence in the confocal images represents particle bound dye. We report observations of changes in the behaviour of MC3T3 cells indicative of the onset of cell death after exposure to labelled SiHA, which correlate with both the size distribution and volume of the material not located within the lysosomes.

SiHA-Lysosome colocalisation was represented by yellow pixels in the overlay confocal microscopy images (†Figure S5 and S6). Analysis of the 3D confocal image stacks revealed that generally no more than approximately 20 μm^3 of material was located within the lysosomes after 24 hours irrespective of the total volume of material in the cells as a whole (which ranged from 20-220 μm^3). No clear relationship was found between the volume of material transferred to lysosomes and the total material internalised by the cell as a whole (figure 1). Three example cases of changes in cell morphology and behaviour are highlighted - 1) cells changing from elongated to a round morphology, 2) an increase in the number of lysosomes and their convergence around internalised structures and, 3) detachment of cells from the substrate. Detachment of cells from the imaging dish suggested late stages of cell death, but there was no clear link between this behaviour and the amount of material located within the lysosomes, which would potentially be a source of dissolved calcium ions. For example, the example case of cell detachment (labelled as '3') in figure 1, was found to contain approximately 215 μm^3 of material within the cell with less than 5 μm^3 of this located within lysosomes. Meanwhile, cells with lysosomes containing up to 45

[a] *Biochemical Engineering, The School of Chemical Engineering, University of Birmingham, Birmingham, UK. *Email: l.m.grover@bham.ac.uk*
† Electronic Supplementary Information (ESI) available: Materials and methods, 1D PAGE images demonstrating , confocal image showing colocalisation and fluorescence spectroscopy data. See DOI: 10.1039/b000000x/

μm^3 of material showed no change in overall morphology.

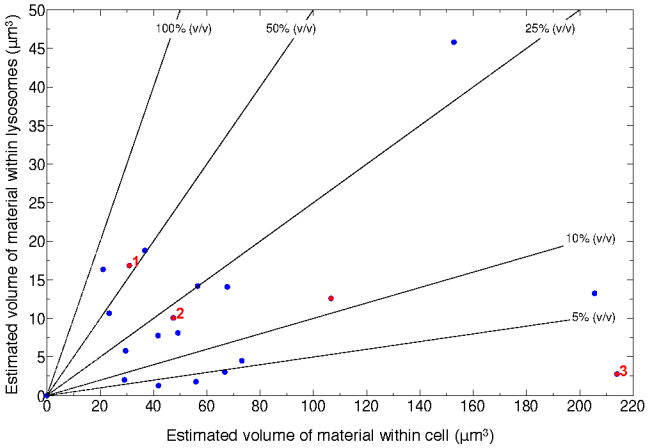

Fig. 1 Scatter plot of total volume of internalised material colocalised within lysosomes against total volume of material within the cell as a whole. There was no clear relationship between how much material was transferred to the lysosomes and the total amount of material within the cell as a whole. Three example cases of changes in cell behaviour are labelled: (1) cell changing from an elongated to round morphology, (2) increase in lysosome number and, (3) cell detachment from substrate.

The distribution of the material within the cells exhibiting changes in morphology and function was then analysed to supplement the volume estimation data. Figure 2 shows size histograms of material detected within (red bars) and outside (blue bars) the lysosomes together with bright field images of example cells showing changes in morphology and confocal fluorescence images of labelled SiHA and lysosomes. Structures up to $1\mu m$ in diameter were most prevalent within the cells, but structures of up to $3-4\mu m$ in diameter were also observed. Lysosomes were generally found to contain structures up to $2-3\mu m$ in diameter, leaving any larger structures within the overall cell. In the case of cell morphology changing from an elongated to a round shapes (figure 2a-d), the majority of all of the material, consisting of structures between $0.2-3\mu m$ in diameter, were taken up by the lysosomes. Total encapsulation of the micron scale material is clearly shown in the orthogonal views of the highlighted region of the fluorescence image where the yellow 'colocalised pixels' are surrounded by the red lysosome. In the second case involving dramatic increase in lysosome recruitment (figure 2e-h), no material with diameter above $2\mu m$ was found within the lysosomes, resulting in approximately 90% of the material remaining within the cytoplasm. Some structures between $2-3\mu m$ were observed to have been partially enclosed by lysosomes (as shown in the inset high magnification fluorescence image) to create a substructure approximately $1.5-2\mu m$ in diameter, which is shown by the creation of a lone red bar within this size class in the size histogram. In this case it can be proposed that the 2-2.5μm size class of structures would eventually become completely encapsulated over time given that structures of up to $3\mu m$ were encapsulated in the first case (a). Nonetheless, the cells which were observed to have increased lysosomal activity contained SiHA structures up to $4\mu m$ in size - none of which were found to colocalise with lysosomes. In the cases where partial cell detachment was observed (figure 2 i-l), no structures larger than $1\mu m$ were detected within the lysosomes (figure 2i) where little colocalisation (yellow coloured pixels) could be seen across the vast majority of the labelled material. Detachment was observed to be a dramatic and rapid process as when by the bright field images (j and k) which were taken approximately 3 minutes apart.

In summary, we have for the first time quantified the volume and size distribution of SiHA located within lysosomes of live MC3T3 cells. Observations of changes in cell morphology and detachment from the surface, which are believed to relate to stages of cell death, 24 hours after exposure to SiHA have been reported and were shown not to depend purely on the total volume of material within the cell as shown in other studies. SiHA aggregates within the cell larger than $1.5\mu m$ not located within lysosomes correlate with onset of cell death. We speculate that the presence of aggregates outside of the lysosome could be the result of: i) the destabilisation of the lysosome membrane due to increased Ca^{2+} ion concentration from the dissolving particle material, thus releasing the undissolved fraction of the particle/aggregate and/or, ii) destabilisation of the late endosomes containing the material before fusion with lysosomes occurs. The latter hypothesis partly stems from the fact that the structures detected outside of the lysosomes exhibited highly localised fluorescence, possibly suggesting that the labelled particles were still intact and therefore had not been subjected to the acidic environment of the lysosomes. However, analysis of the local free Ca^{2+} ion distribution around these regions and labelling of late endosomes may be required to fully investigate this theory. Understanding the mechanism of escape will be the focus of our future work in this area. These results may have wider implications for the understanding of how particles eroded from the surface of implants may influence biological response and highlight that biological response even to non-toxic materials may be strongly size dependent. This presents an additional important consideration for the design of new implant materials.

We would like to acknowledge the funding for this work provided by the EPSRC (grant reference: EP/F50053X/1). We would also like to acknowledge Advantage West Midlands and the Birmingham Advanced Light Microscopy centre for the provision of and access to the confocal microscope used in this work.

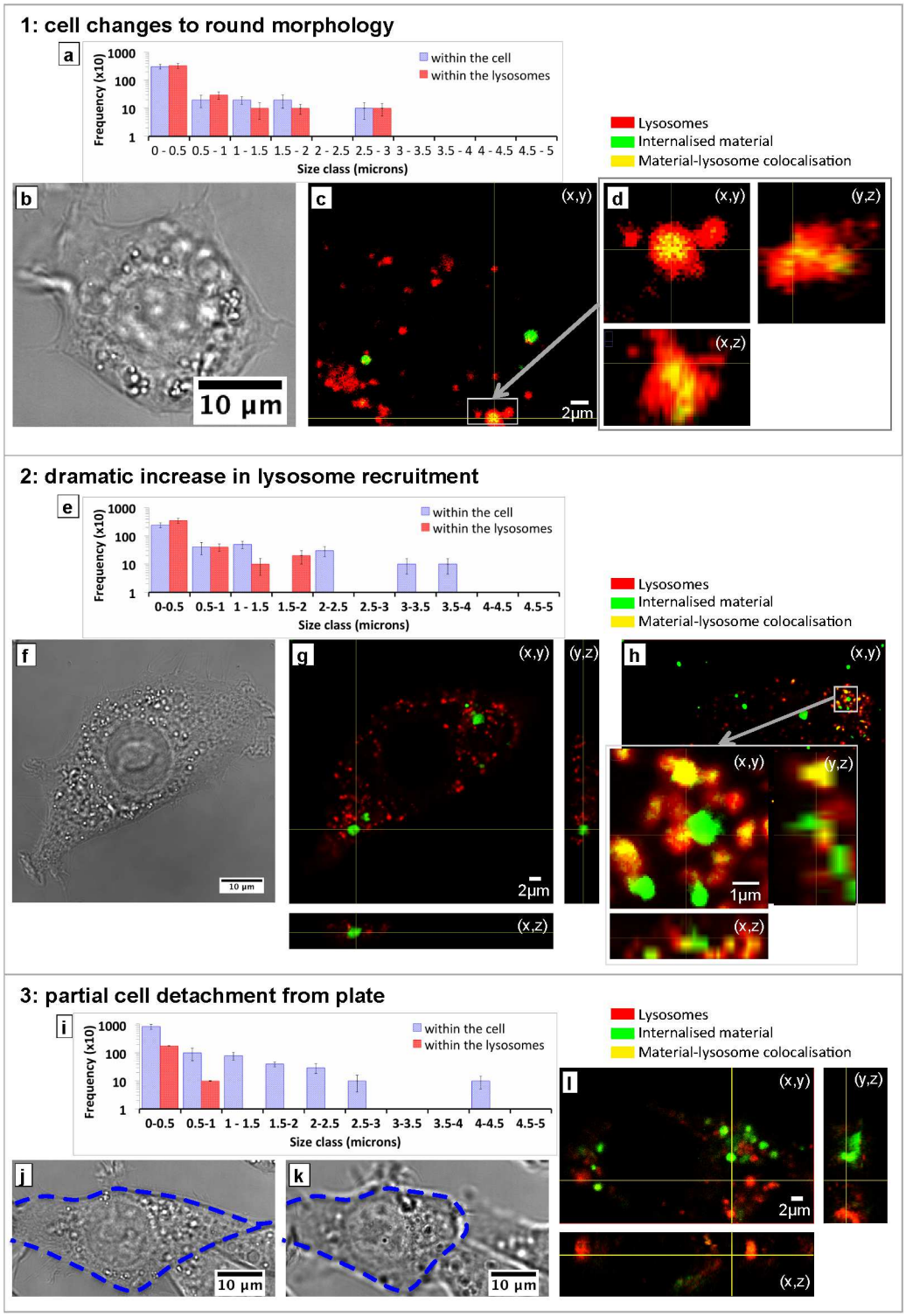

Fig. 2 Three example cases of changes in cell behaviour, which correlated with location of the internalised material within the cell. In each of the three cases, a size distribution of material inside the cell and within the lysosomes (a; e; i), bright field images showing the changes in cell morphology (b; f; j,k) and confocal fluorescence images (c,d; g,h; l) are presented. Histograms scaled by factor 10 and shown on a Log-10 scale for clarity and the error bars represent standard deviation of the size measurements. Structures larger than $1 - 1.5\mu$m not encapsulated within lysosomes appear to correlate with the observations of cell death suggesting an interplay between total amount and size distribution of CaP internalised on cell fate.

References

1 V. Sokolova, A. Kovtun, O. Prymak, W. Meyer-Zaika, E. A. Kubareva, E. A. Romanova, T. S. Oretskaya, R. Heumann and M. Epple, *J. Mater. Chem.*, 2006, **17**, 721–727.

2 C. Ribeiro, C. Barrias and M. Barbosa, *Biomaterials*, 2004, **25**, 4363–4373.

3 S. J. Kalita, A. Bhardwaj and H. A. Bhatt, *Materials Science and Engineering: C*, 2007, **27**, 441–449.

4 J. Klesing, S. Chernousova and M. Epple, *Journal of Materials Chemistry*, 2012, **22**, 199–204.

5 S. C. Lee, H. W. Choi, H. J. Lee, K. J. Kim, J. H. Chang, S. Y. Kim, J. Choi, K.-S. Oh and Y.-K. Jeong, *Journal of Materials Chemistry*, 2007, **17**, 174–180.

6 K. Ganesan, A. Kovtun, S. Neumann, R. Heumann and M. Epple, *J. Mater. Chem.*, 2008, **18**, 3655–3661.

7 L. Chen, J. M. Mccrate, J. C. Lee and H. Li, *Nanotechnology*, 2011, **22**, 105708.

8 M. Motskin, D. Wright, K. Muller, N. Kyle, T. Gard, A. Porter and J. Skepper, *Biomaterials*, 2009, **30**, 3307–3317.

9 Y. Yuan, C. Liu, J. Qian, J. Wang and Y. Zhang, *Biomaterials*, 2010, **31**, 730–740.

10 M. Motskin, K. H. Müller, C. Genoud, A. G. Monteith and J. N. Skepper, *Biomaterials*, 2011, **32**, 9470–9482.

11 S. Orrenius, B. Zhivotovsky and P. Nicotera, *Nature Reviews Molecular Cell Biology*, 2003, **4**, 552–565.

12 M. P. Mattson and S. L. Chan, *Nature cell biology*, 2003, **5**, 1041–1043.

13 G. Hajnóczky, G. Csordás, S. Das, C. Garcia-Perez, M. Saotome, S. Sinha Roy and M. Yi, *Cell calcium*, 2006, **40**, 553–560.

14 R. L. Williams, M. J. Hadley, P. J. Jiang, N. A. Rowson, P. M. Mendes, J. Z. Rappoport and L. M. Grover, *J. Mater. Chem. B*, 2013, **1**, 4370–4378.